Raman and x-ray studies of a high-pressure phase transition in β-$LiIO_3$ and the study of anharmonic effects

J. Mendes Fílho, V. Lemos, F. Cerdeira, and R. S. Katiyar
Instituto de Fisica "Gleb Wataghin," Universidade Estadual de Campinas, 13 100 Campinas, São Paulo, Brazil

R. M. Hazen and L. W. Finger
Geophysical Laboratory, Carnegie Institution of Washington, Washington, D.C. 20008
(Received 8 June 1984)

Temperature- and pressure-dependent Raman scattering experiments have been performed to study the phonon behavior in β-$LiIO_3$. The temperature dependence of Raman-active phonons does not show anomalous frequency behavior in the temperature range 10—650 K; however, at least two B_g phonons, with frequencies 344 and 460 cm^{-1}, and one A_g phonon, with frequency 249 cm^{-1}, show anomalous increases in linewidth with temperature. The high-pressure Raman scattering experiments of β-$LiIO_3$ were performed at room temperature with a sapphire-anvil cell for hydrostatic pressures up to 95 kbar. The spectra show a discontinuous reversible change for all orientations at about 50 kbar. This change is interpreted as a phase transition in $LiIO_3$ at 50 kbar. The Raman spectra of this new δ phase are quite different from those of the three other known phases of $LiIO_3$ and reveal a lowering of symmetry upon passing from the β to the δ phase. High-pressure x-ray measurements were performed to characterize the structural phase transition in β-$LiIO_3$, which transforms from tetragonal symmetry $P4/n$ (C_{4h}^3) to monoclinic symmetry $P2/n$ (C_{2h}^4) above 50 kbar. The complex behavior at high pressure appears to be analogous to that of some perovskite compounds, in which there exists an antipathetic lattice coupling between a and c of a tetragonal phase. The pressure and temperature dependence of Raman spectra of β-$LiIO_3$ were combined to analyze the explicit and implicit contributions to the isobaric temperature variation of phonons. The results show that at least two modes, the B_g phonon at 460 cm^{-1} and the A_g phonon at 249 cm^{-1}, are highly anharmonic with increasing temperature. It is concluded from pressure Raman work that there exists strong mixing of internal and external modes in β-$LiIO_3$. Such a mixing of internal- and external-mode characters is also apparent from the study of fractional implicit and explicit contributions to the frequency variations of phonons with temperature.

I. INTRODUCTION

The utility of pressure- and temperature-dependent Raman scattering to study anharmonic effects in solids is now well recognized.[1,2] The anharmonic terms in the crystal potential energy account for not only the finite lifetime of the phonons (γ^{-1}) but also the shift in the normal-mode frequencies (Δ); for example, the well-known soft-mode behavior in displacive ferroelectrics.[3] The anharmonicity can be expressed as a complex quantity in the self-energy expression, i.e., $\Sigma=\Delta-i\gamma$. The real part gives the measured, renormalized soft-mode frequency ω_0, which can be written as $\omega_0^2=\Omega_0^2+2\Omega_0\Delta$, where Ω_0 is the pure harmonic frequency. The imaginary part γ determines the phonon damping constant Γ, which is related to γ by the equation $\gamma=\omega\Gamma/2\Omega_0$. In lowest-order perturbation theory, γ receives contributions from cubic anharmonicities[4,5] (second order), whereas the contributions to Δ can be divided into $\Delta_E+\Delta_3+\Delta_4$, where Δ_E represents the frequency shift produced by thermal expansion, and Δ_3 and Δ_4 are the contributions of cubic and quartic anharmonicities, respectively.

A principal objective of this study was to determine anharmonic contributions in β-$LiIO_3$ through an investigation of pressure- and temperature-dependent Raman scattering. The pressure and temperature dependence of the phonon frequencies are combined to separate the implicit (volume-driven) and explicit (occupation-number-driven) contributions to the latter.[1] Such a procedure has been applied to a large variety of materials to determine the nature of anharmonic contributions and to correlate them with the anomalous behavior of several physical properties and possible structural phase transitions in materials.

In a recent paper, Lemos *et al.*[6] reported pressure-dependent Raman scattering in β-$LiIO_3$. Analysis of the results showed that the crystal undergoes an abrupt reversible structural phase transition to a new, unknown phase at about 50 kbar hydrostatic pressure. A second objective of this study, therefore, is to characterize structural aspects of the β-$LiIO_3$ phase transition with high-pressure x-ray-diffraction techniques and to measure the compressibility of the material in its two phases.

II. EXPERIMENTAL DETAILS

The crystals of β-$LiIO_3$ are grown from an aqueous solution at temperatures greater than 75 °C.[7,8] The crys-

TABLE I. Unit-cell parameters of β-$LiIO_3$ at several pressures.

Pressure (kbar)	a (Å)	b (Å)	c (Å)	γ (deg)	V (Å^3)
0.001	9.722(1)	9.725(1)	6.1517(1)	90.01(1)	581.61(4)
10.8	9.539(1)	9.543(1)	6.1583(3)	89.97(1)	560.60(12)
13.1	9.510(2)	9.515(2)	6.159(1)	90.00(2)	555.4(2)
23.0	9.369(4)	9.369(4)	6.160(2)	90.00(5)	540.7(5)
35.8	9.241(5)	9.238(5)	6.151(2)	90.04(3)	525.1(5)
45.3	9.160(3)	9.158(3)	6.130(2)	89.98(3)	514.2(3)
50.2	9.097(2)	9.088(3)	6.122(1)	89.95(2)	506.1(2)
54.9	9.050(1)	9.035(2)	6.107(1)	90.10(1)	499.4(1)
59.0	9.008(1)	8.996(1)	6.0985(2)	90.05(1)	494.19(9)
62.0	8.990(2)	8.974(2)	6.092(4)	90.02(2)	491.5(2)
63.7	8.969(3)	8.960(4)	6.085(4)	90.00(2)	489.0(4)

tals are stable at room temperature and do not transform into the α or γ phase over the range of temperatures and pressures studied. Moreover, unlike the α phase, β-$LiIO_3$ does not possess any piezoelectric or nonlinear-optical properties.

Pressure Raman experiments, described in detail by Lemos *et al.*,[6] were performed in an opposed-anvil cell with one anvil made of sapphire.[9] The 5145-Å radiation of an argon-ion laser was used as the exciting radiation. The scattered light was analyzed with a SPEX double monochromator equipped with photon-counting detection.

The low-temperature (10—300 K) Raman measurements were performed with a cold finger of a closed-cycle, liquid-helium Dewar from Air Products, Inc. (DISPLEX system) with an automatic temperature control controllable to an accuracy of ± 0.5 K. Single crystals in the form of parallelopipeds ($\approx 4\times 4\times 3$ mm), with the shortest dimension along the crystallographic c axis, were cut and polished for such measurements. The samples were glued with General Electric varnish onto the cold finger of the Dewar. The Raman spectra were recorded in various scattering configurations. For high-temperature measurements the sample was placed inside a homemade cylindrical oven with glass windows. The temperature was controlled within ± 1 °C with an Artronix temperature controller (model 5301-E).

Samples for high-pressure x-ray studies were cut from the specimen used for Raman scattering measurements. A flat crystal fragment, measuring approximately $100\times 100\times 25$ μm, was mounted in a diamond-anvil pressure cell for single-crystal, x-ray-diffraction studies.[10] Ruby fragments were included in the mount for pressure calibration.[11] Unit-cell dimensions were measured at 11 pressures between 1 bar and 64 kbar; the procedure of King and Finger[12] was employed. Unit-cell parameters for β-$LiIO_3$ at several pressures are reported in Table I.

The Raman spectra of β-$LiIO_3$ were recorded at several temperatures between 10 and 650 K in the configuration $Y(XZ)X$ (E_g modes), $Y(XY)X$ (B_g modes), and $Y(ZZ)X$ (A_g modes). Plotted in Fig. 1 are four spectra taken at different temperatures for each scattering configuration. The peaks corresponding to normal modes are best identified in the spectra at 10 K. Unambiguous assignment of peaks for various symmetries was determined from the temperature dependence. In all, 15 peaks were identified corresponding to B_g symmetry, 14 peaks corresponding to E_g symmetry, and 13 peaks corresponding to A_g symmetry, compared with 15 modes for each symmetry predicted by group theory.[13] The frequencies of these modes are listed in Table II. The linewidth for most of these modes increases with temperature, and some of the peaks fuse into neighboring peaks, thus producing broader structures at higher temperatures.

Raman spectra of β-$LiIO_3$ were recorded at several pressures up to 95 kbar at room temperature. Some of the typical spectra for symmetries A_g, B_g, and E_g are illustrated in Fig. 2. The Raman spectra in all configurations show smooth variation in their peaks for pressures up to 48 kbar, but they change discontinuously at a pressure of 50 kbar.

III. ANALYSIS OF RAMAN SPECTRA

The space-group symmetry of β-$LiIO_3$ is $P4_2/n$ (C_{4h}^4) with eight formula units in the unit cell.[7] The unit-cell dimensions at room temperature are $a=9.712$ Å and

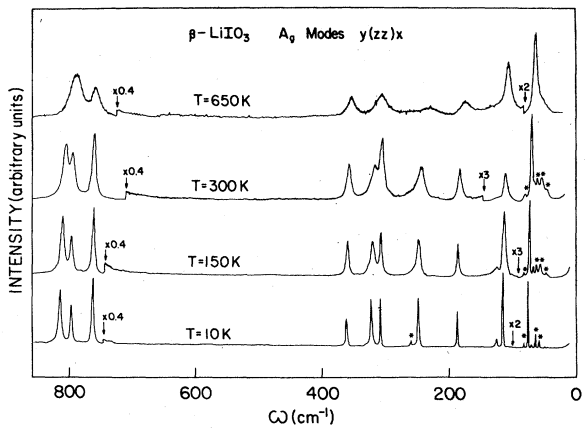

FIG. 1. Raman spectra of β-$LiIO_3$ taken with $Y(ZZ)X$ at several temperatures. Asterisks indicate "leaks" from forbidden symmetries.

TABLE II. Phonon frequencies and half-widths (given in parentheses) for Raman-active species in β-$LiIO_3$.

Number	A_g $\omega(\Gamma)$ (cm^{-1})	B_g $\omega(\Gamma)$ (cm^{-1})	E_g $\omega(\Gamma)$ (cm^{-1})
1	69.3 (1.2)	48.7 (1.0)	58.5 (1.2)
2	75.9 (1.2)	56.6 (1.4)	64.4 (1.2)
3	116.0 (1.8)	108.1 (1.6)	82.4 (1.2)
4	126.3 (1.8)	125.1 (2.0)	105.5 (1.8)
5	188.3 (1.8)	149.3 (1.4)	148.8 (1.8)
6		232.0 (1.6)	227.2 (1.8)
7	249.1 (2.4)	260.7 (2.0)	260.7 (2.4)
8		294.5 (3.8)	283.5 (4.8)
9	308.5 (2.0)	303.5 (1.6)	308.5 (1.8)
10	322.5 (3.2)	320.2 (5.0)	330.6 (2.6)
11	361.8 (2.4)	344.7 (4.0)	386.5 (5.4)
12	442.0 (6.0)	460.6 (8.0)	
13	763.8 (3.2)	776.9 (5.0)	766.5 (3.2)
14	798.3 (3.6)	783.1 (3.4)	783.7 (4.4)
15	816.3 (5.2)	816.9 (5.0)	825.7 (4.4)

$c=6.146$ Å.[14] The structure consists of discrete IO_3^- groups in the form of distorted trigonal pyramids with three longer I—O bonds defining very distorted iodine octahedra, and distorted LiO_4 tetrahedra, each of which is corner-linked to two other tetrahedra. Helical groups of iodine "octahedra" form chains parallel to the c axis. These chains are rigid in the c-axis direction, but are relatively weakly cross-linked in the (001) plane. Thermal-expansion studies by Schulz[14] showed very anisotropic behavior with expansion of the a axis 20 times that of the c axis.

The zone-center optical phonons in β-$LiIO_3$ are distributed as

$$15A_g+15B_g+15E_g+14A_u+14E_u+15B_u\ .$$

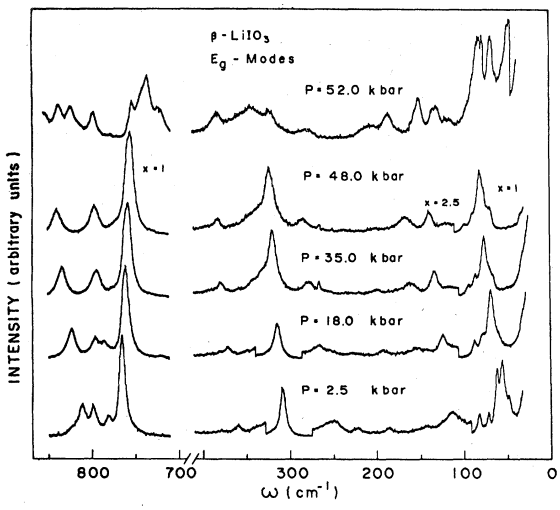

FIG. 2. Raman spectra of E_g modes of β-$LiIO_3$ taken at different pressures. A discontinuous, reversible change between pressures of 48 and 52 kbar is an indication of structural transition.

The modes belonging to the symmetries A_g, B_g, and E_g are Raman active, those belonging to A_u and E_u are infrared active, and the B_u modes are inactive in both Raman and infrared spectra. These modes can be classified further into external vibrations due to Li^+ and IO_3^- units and internal vibrations of the IO_3^- group. Three modes predominantly due to I—O stretching and three bending modes are thus expected for each symmetry. Moreover, there should be six translatory-type and three rotatory-type vibrational modes in the external frequency region. Preliminary lattice-dynamical calculations show that the external vibrations are well mixed with the internal vibrations of deformation type. The stretching modes of the IO_3^- group are, however, practically pure. The two stretching frequencies ν_1 and ν_3 of the free IO_3^- ion are 779 and 826 cm^{-1}.[15] In the crystal phase of β-$LiIO_3$ the degeneracy of the ν_3 mode is lifted and three IO_3 stretching modes belonging to each symmetry species appear. The free-ion bending modes (ν_2 and ν_4 with frequencies of 390 and 330 cm^{-1}) lose their character and mix with Li—O_4 vibrations, unlike in α-$LiIO_3$.[16] On the basis of lattice-dynamical calculations an attempt was made to establish the dominant character of modes appearing in the region below 500 cm^{-1}, and the results are presented in Table III. Accordingly, the modes at 344.7 and 460.6 cm^{-1} of B_g symmetry possess considerable Li—O stretching character. The modes with frequencies below 140 cm^{-1} are primarily the result of vibrations of IO_3^- groups as a whole. Such an identification of mode character was achieved by carrying out a least-squares fit of most of the observed frequencies to a rigid-ion model with short-range axially symmetric and long-range Coulomb forces. This procedure was similar to that applied to lead titanate by Katiyar and Freire.[17]

The temperature dependence of frequencies and linewidth of several modes belonging to different symmetries in β-$LiIO_3$ are plotted in Figs. 3 and 4. It has been difficult to analyze the spectra taken at higher temperatures because of the broadening and fusing of various modes. From Fig. 3 it can be seen that the overall temperature dependence of frequencies of normal modes is linear with temperature; however, linewidths (see Fig. 4) of modes at 249.1 cm^{-1} belonging to A_g symmetry and of modes at 344.7 and 460.6 cm^{-1} of B_g symmetry increase nonlinearly with increasing temperature. Such an increase in linewidths results from the anharmonic contributions to the normal modes in β-$LiIO_3$.

The pressure dependence of Raman modes, identifiable at room temperature, was studied up to 95 kbar. As reported previously,[6] the spectra change discontinuously at a hydrostatic pressure of about 50 kbar, thereby revealing a possible phase transition in β-$LiIO_3$. Frequencies of the modes below the transition pressure were analyzed for all Raman-active species.[6] Only seven out of 18 modes studied show a nonlinear variation in frequency with pressure. All these modes, except one stretching mode at 793.3 cm^{-1} belonging to A_g symmetry, lie in the frequency region below 500 cm^{-1}. None of the E_g modes show non-

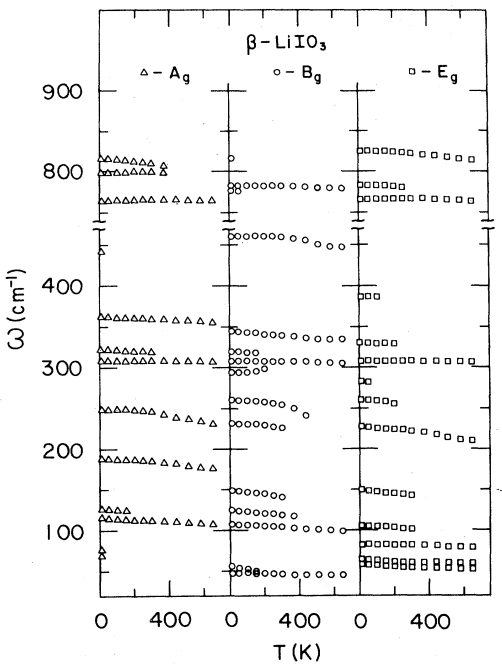

FIG. 3. Temperature dependence of phonon frequencies for different symmetries.

linear behavior. The two B_g modes with nonlinear behavior are at 48.7 and 149.3 cm^{-1}. It is interesting to note that the frequencies of all the modes in the frequency region below 500 cm^{-1} increase with pressure. The lowest stretching modes (near 770 cm^{-1}) in all symmetries, however, soften with pressure.

The temperature variation of mode frequency can be related to the variation of the mode frequency with pressure and, for anisotropic materials, can be written as follows:

$$\left[\frac{\partial\omega_j}{\partial T}\right]_P = -\frac{\beta}{K}\left[\frac{\partial\omega_j}{\partial P}\right]_T + \left[\frac{\partial\omega_j}{\partial T}\right]_V + \alpha_j$$
$$= -\beta\omega_j\gamma_j + \left[\frac{\partial\omega_j}{\partial T}\right]_V + \alpha_j \ , \quad (1)$$

where the volume thermal expansion $\beta = 2\beta_{\underline{a}} + \beta_{\underline{c}}$, the volume compressibility $K = 2K_{\underline{a}} + K_{\underline{c}}$, and γ_j is the mode-Grüneisen parameter. The subscripts $\underline{a}$ and $\underline{c}$ refer to the crystallographic axes.

The first term on the right-hand side of (1) represents the implicit contribution, which arises from thermal expansion through the volume dependence of the phonon frequency. The second term is known as the explicit contribution, and it is produced by the change in vibrational amplitude (phonon occupation number) accompanying the temperature variation. The anisotropic constant, α_j for mode j, may be expressed in terms of deformation-potential constants following the procedure for α-$LiIO_3$ by Cerdeira *et al.*[2] The term for α_j can be written as

$$\alpha_j = (2/K)(\beta_{\underline{a}}K_{\underline{c}} - \beta_{\underline{c}}K_{\underline{a}})(a_j - b_j) \ . \quad (2)$$

In order to calculate the value of α_j, it is necessary to perform Raman experiments on crystals under uniaxial pressure for determining a_j and b_j. No such study, however, has been reported in the literature for β-$LiIO_3$. For α-$LiIO_3$ it has been shown by Cerdeira *et al.*[2] that α_j is negligibly small compared with the first term, $\beta\omega_j\gamma_j$, on the right-hand side of Eq. (1), for all modes. Such an approximation should also be valid for β-$LiIO_3$.

In order to analyze the temperature and pressure dependence of phonon frequencies in β-$LiIO_3$, the above equation may be integrated for a finite interval of temperature. Such an integration would require knowledge of the temperature dependence of the thermal-expansion coefficient β and the compressibility K. In the absence of any such study in the literature, the analysis is limited to measurements above a certain cutoff temperature T_0, where it is assumed that both β and K remain approximately constant. Cerdeira *et al.*[2] determined that $T_0 = 50$ K for α-$LiIO_3$. The room-temperature value of β was given by Matsumura[7] as 6.77×10^{-5} K^{-1}, and from x-ray data a value of $K = 3.33\times10^{-3}$ $kbar^{-1}$ is obtained. Equation (1) can thus be written in terms of finite differences as follows:

$$(\Delta\omega_T)_P = -(\Delta\omega_P)_T + (\Delta\omega_T)_V \ , \quad (3)$$

where

$$(\Delta\omega_T)_P = -[\omega_j(T) - \omega_j(T_0)]_P \ ,$$
$$(\Delta\omega_T)_V = [\omega_j(T) - \omega_j(T_0)]_V \ ,$$

and

$$(\Delta\omega_P)_T = \frac{\beta}{K}\left[\frac{\partial\omega_j}{\partial P}\right]_T (T - T_0) \ . \quad (4)$$

The quantities $(\Delta\omega_T)_P$ and $(\Delta\omega_P)_T$ in the above equations can be obtained from experimental Raman data.

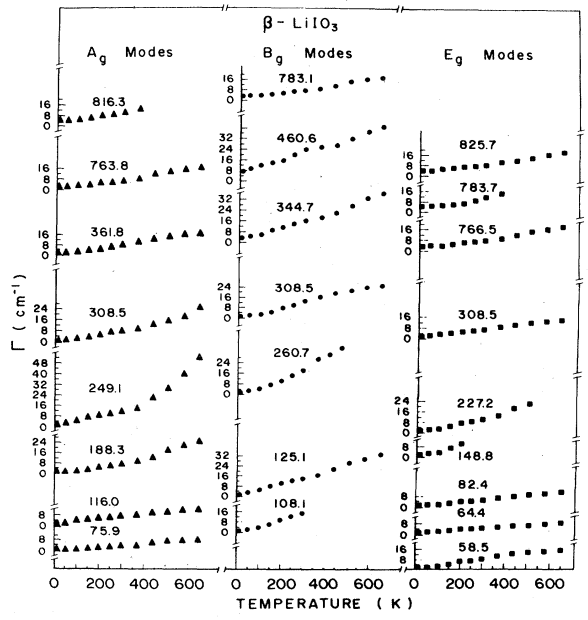

FIG. 4. Full width at half maximum of the Raman lines vs temperature. The frequency values are taken from the spectra at 10 K.

The explicit contribution $(\Delta\omega_T)_V$ to the variation of phonon frequency with temperature can then be calculated. Plotted in Fig. 5 is the temperature dependence of such explicit contributions for phonons of Raman-active symmetries. These are shown by solid circles, triangles, and squares. The heavy solid lines show the implicit contribution, $-(\Delta\omega_P)_T$, for each phonon. The horizontal lines indicate the base line in each case. It may be noted that, among the modes studied, the A_g mode at 249.1 cm^{-1} and the B_g mode at 460.6 cm^{-1} show a larger change in the explicit contribution with increasing temperature as compared with implicit contributions. This behavior is in contrast to that observed in α-$LiIO_3$ for external modes,[2] where implicit contributions largely dominate the temperature dependence of the external phonons. The abnormal behavior of modes at 249.1 and 460.6 cm^{-1} is the indication of large anharmonicities involved in the description of these modes. Such an interpretation is not possible from a study only of the temperature dependence of phonon frequencies, because of implicit and explicit contributions acting in opposite directions and thus partially canceling the temperature dependence.

The information displayed in Fig. 5 can also be analyzed quantitatively by comparing both temperature and pressure variation of phonon frequencies in the differential form of Eq. (1). This analysis is given in Table III, in which the terms appearing in this equation are listed explicitly. The results are also plotted in Fig. 6, where solid circles, triangles, and squares represent stretching modes in all symmetries. In Table III the quantities η and θ represent the fractional implicit and explicit contributions to the isobaric temperature derivatives. The observed trends in these quantities, as well as the mode-Grüneisen parameter for a large variety of ionic, covalent, and molecular crystals, are reviewed by Weinstein and Zallen.[1] They concluded that the mode-Grüneisen parameter γ_j may be expressed as a function of the mode frequency, i.e., $\gamma_j \sim \omega^{-n}$. For ionic or covalent materials such as NaCl and diamond, $n=0$, i.e., γ_j is frequency independent. For molecular solids such as As_4S_4 and Pb_4S_3, the value of n equals 0 for external modes (in this case the modes have very low frequencies), and n equals 2 for internal modes of the molecules. In these materials a large gap exists between the external and internal modes. It has also been observed that, for several other molecular or ionic molecular materials, such as S_8 and As_2S_3, where the separation between the external and internal vibrations is less clear cut, the value of n for all modes is approximately 2. This latter vibration behavior is the case for α-$LiIO_3$ as well.[2]

Lemos *et al.*[6] obtained a value of $n=1.3$ for β-$LiIO_3$ and, moreover, they used the data of Peercy *et al.*[18] to derive $n=1$ for TeO_2. In both of these cases the internal and external modes could not be clearly separated. It appears that the mixing of external and internal modes reduces n from 2; this deviation from 2 could provide a measure of the external- and internal-mode mixing.

In regard to fractional contributions η and θ to frequency variation with temperature, Weinstein and Zallen[1] have concluded that for ionic crystals thermal expansion dominates ($n \approx 1$), whereas in tetrahedrally coordinated

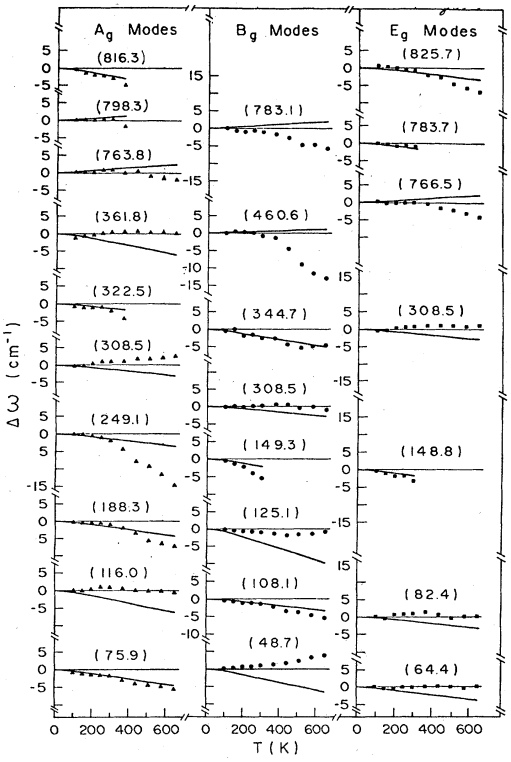

FIG. 5. Implicit, $-(\Delta\omega_P)_T$, and explicit, $(\Delta\omega_T)_V$, contributions to the frequency shift as a function of temperature. Solid lines, implicit contributions; solid circles, explicit contributions.

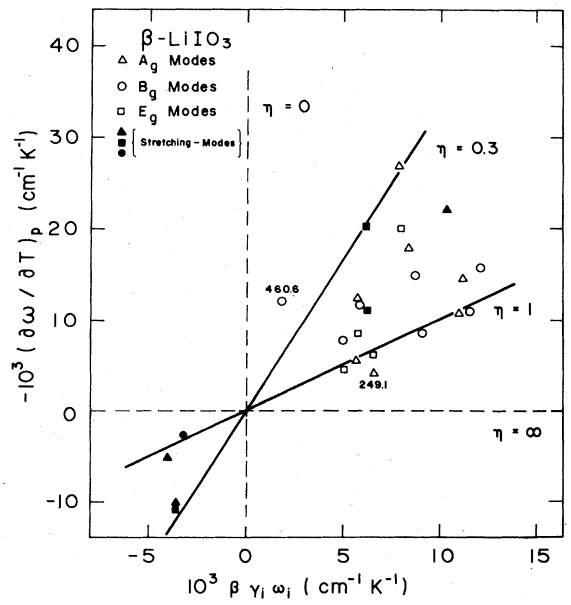

FIG. 6. Implicit vs explicit temperature derivatives for the Raman-active modes of β-$LiIO_3$. Lines of constant fractional implicit contribution (η) are shown for comparison with the data (triangles, circles, and squares). The solid symbols denote internal stretching modes for the IO_3 group.

TABLE III. Mode frequencies, Grüneisen parameters, and the temperature derivatives of mode frequencies separated into their implicit and explicit components. η and θ are fractional values of these components, respectively.

Symmetry	ω_j (cm^{-1}) (at 10 K)	γ_j	$\left[\frac{\partial\omega_j}{\partial T}\right]_P$	$-\beta\omega_j\gamma_j$ (10^{-3} cm^{-1}K^{-1})	$\left[\frac{\partial\omega_j}{\partial T}\right]_V$	η	θ	Normal-mode character
A_g	75.9	1.73	−17.8	−10.3	−7.5	0.58	0.42	IO_3–IO_3
	116.0	1.46	−14.5	−13.7	−0.8	0.95	0.05	IO_3–IO_3
	188.3	0.63	−26.3	−9.7	−17.1	0.36	0.64	mixed
	249.1	0.39	−4.1	−7.9	3.9	1.93	0.93	Li–IO_3
	308.5	0.28	−5.7	−5.8	0.1	1.02	0.02	mixed
	322.5	0.27	−12.3	−7.1	−5.2	0.58	0.42	mixed
	361.8	0.45	−10.7	−13.3	2.6	1.24	−0.24	Li–O translational vibration
	763.8	−0.07	11.7	4.4	7.3	0.37	0.63	IO_3 stretching
	798.3	−0.07	5.1	4.9	0.2	0.96	0.04	IO_3 stretching
	816.3	0.19	−22.0	−12.9	−9.1	0.59	0.41	IO_3 stretching
B_g	48.7	3.69	−11.4	−14.3	2.9	1.25	−0.25	IO_3–IO_3
	108.1	0.83	−11.6	−7.3	−4.3	0.63	0.37	IO_3–IO_3
	149.3	0.95	−8.5	−11.1	2.6	1.30	−0.31	mixed
	308.5	0.24	−7.8	−6.1	1.7	0.78	0.22	mixed
	344.7	0.38	−14.9	−8.1	−6.8	0.54	0.46	Li–O translational vibration
	460.6	0.05	−12.5	−2.2	−10.3	0.17	0.83	Li–O translational vibration
	783.1	−0.06	2.9	3.1	0.2	1.06	−0.06	IO_3 stretching
E_g	64.4	1.57	−6.0	−8.1	2.1	1.35	−0.35	IO_3–IO_3
	82.4	1.04	−8.5	−7.1	−1.4	0.84	0.16	IO_3–IO_3
	148.8	0.83	−20.0	−9.9	−10.1	0.50	0.50	mixed
	308.5	0.25	−5.2	−6.5	2.1	1.25	−0.25	mixed
	766.5	−0.07	11.0	4.4	6.6	0.40	0.60	IO_3 stretching
	783.7	0.12	−11.0	−7.9	−3.1	0.72	0.28	
	825.7	0.11	−24.0	−7.3	−16.7	0.30	0.70	

semiconductors (covalent bonding) a value of $\eta \approx 0.3$ is typical. In molecular solids, $\eta = 1$ for well-separated external modes, but the internal modes have values of η characteristic of covalent bonding ($\eta \approx 0.3$). In any other case the values of η should fall within the above limits. Such analysis, however, is valid only if the anharmonic contributions to the mode frequency are small. When these conclusions are applied to Fig. 6, it is evident that even the well-separated internal stretching modes have values of η spread over the range 0.3 to 1. Other internal modes possess entirely mixed character. All modes except the B_g mode at 460.6 cm^{-1} ($\eta = 0.17$) and the A_g mode at 249.1 cm^{-1} ($\eta = 1.9$) fall inside the limit $\eta = 0$ to 1.0. Both of these modes possess highly anharmonic contributions and predominantly involve motion of Li ions against oxygen ions. The role of these modes in the newly discovered phase transition at ~50 kbar could not, however, be established. For such an analysis, it is necessary to determine the pressure dependence of infrared-active modes and the acoustic modes as well.

IV. ANALYSIS OF X-RAY MEASUREMENTS

Compression of lithium iodate is unusual because the *c* axis expands with increasing pressure between 1 bar and 20 kbar (Fig. 7); however, the *a* axes compress significant-

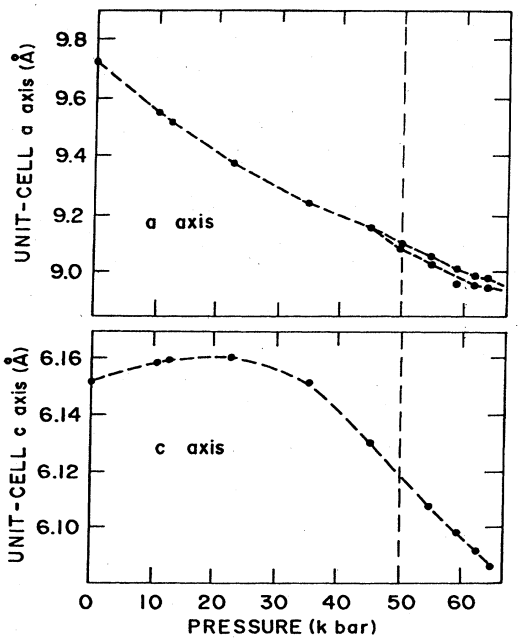

FIG. 7. Pressure dependence of unit-cell axes *a* and *c*. The vertical dashed line denotes the transition pressure.

ly. The net changes result in the required positive bulk compressibility (0.0033 $kbar^{-1}$). Compressibility of the $\underline{c}$ axis increases continuously from $-0.000\,10$ $kbar^{-1}$ at 1 bar to $0.000\,41$ $kbar^{-1}$ at 50 kbar, whereas the compressibility of the $\underline{a}$ axis decreases from $0.000\,17$ to $0.000\,08$ $kbar^{-1}$ over this same pressure range. The axial compression behavior of β-$LiIO_3$ implies a strong coupling of bonding between the $\underline{a}$ and $\underline{c}$ axes. As polyhedra distort with increasing pressure, bonding in the (001) plane becomes stronger at the expense of bonding parallel to the iodate helices.

A decrease in dimensional symmetry from tetragonal to monoclinic is observed at the 50-kbar transition. The axes perpendicular to $\underline{c}$ become slightly different in length [$(0.20\pm0.02)\%$ at 62 kbar], and the angle γ deviates by up to 0.1° from the ideal tetragonal angle of 90°. No volume change is observed at the transition, although a volume discontinuity less than 0.2% is not ruled out by these pressure-volume data.

A significant change in compression behavior is observed at (50 ± 5) kbar. The compressibility of the $\underline{c}$ axis decreases, whereas that of the $\underline{a}$ and $\underline{b}$ axes in the (001) plane increases. Furthermore, the compression of one axis in the (001) plane appears to be slightly greater than that of the other; thus, deviations from tetragonality seem to increase slightly with pressure. An inflection in the pressure-volume curve is observed at the transition.

The structure of the monoclinic form of β-$LiIO_3$ is only slightly distorted from that of the tetragonal phase; the space group of the high-pressure form (in the same orientation as the tetragonal unit cell) is $P2/c$ (C_{2h}^4) which is a subgroup of the tetragonal symmetry and is an alternative setting of space group $P2/b$ (C_{2h}^4). This transition thus meets all requirements for a second-order, reversible phase transformation. It is also possible, given the strong structural coupling between the $\underline{a}$ and $\underline{c}$ axes of the tetragonal phase, that the β-$LiIO_3$ transition is ferroelastic (i.e., it can be induced by an applied stress). The complex behavior of $LiIO_3$ at high pressure may thus be analogous to that of some perovskite-type compounds, in which coupling between mutually perpendicular directions leads to reversible ferroelectric transitions. Further studies on the behavior of elastic properties at this phase transition are warranted on the basis of the present structural data.

ACKNOWLEDGMENTS

Financial support provided by Fundação de Amparo à Pesquisa do Estado de São Paulo and Conselho Nacional de Desenvolvimento Científico e Tecnológico to carry out this work is gratefully acknowledged. High-pressure x-ray studies were supported by the National Science Foundation (U.S.) under Grant No. EAR-81-15517. We are grateful to Professor O. L. Alves, Inorganic Chemistry Department, who grew the samples of β-$LiIO_3$ used in our experiments.

[1]B. A. Weinstein and R. Zallen, Top. Appl. Phys. **54**, 463 (1980).

[2]F. Cerdeira, F. E. A. Melo, and V. Lemos, Phys. Rev. B **27**, 7716 (1983).

[3]W. Cochran and R. A. Cowley, in *Handbuch der Physik,* edited by S. Flügge and L. Genzel (Springer, Berlin, 1967), Vol. 25, Pt. 2a, p. 59.

[4]A. Maradudin and E. Fein, Phys. Rev. **128**, 2589 (1962).

[5]R. A. Cowley, Philos. Mag. **11**, 673 (1965); Adv. Phys. **12**, 421 (1963).

[6]V. Lemos, J. Mendes Fílho, F. E. A. Melo, R. S. Katiyar, and F. Cerdeira, Phys. Rev. B **28**, 2985 (1983).

[7]S. Matsumura, Mater. Res. Bull. **6**, 469 (1971).

[8]O. L. Alves and J. Mendes Fílho (unpublished).

[9]R. S. Hawke, K. Syassen, and W. B. Holzapfel, Rev. Sci. Instrum. **45**, 1593 (1974).

[10]R. M. Hazen and L. W. Finger, *Comparative Crystal Chemistry* (Wiley, New York, 1982).

[11]G. J. Piermarini and S. Block, Rev. Sci. Instrum. **46**, 973 (1975); J. D. Barnett, S. Block, and G. J. Piermarini, *ibid.* **44**, 1 (1973).

[12]H. E. King and L. W. Finger, J. Appl. Crystallogr. **12**, 374 (1979).

[13]J. Mendes Fílho, V. Lemos, and F. Cerdeira, Solid State Commun. **45**, 331 (1983).

[14]H. Schulz, Acta Crystallogr. Sect. B **29**, 2285 (1973).

[15]W. E. Dasent and R. C. Waddington, J. Chem. Soc. **20**, 2429 (1960).

[16]F. E. A. Melo, F. Cerdeira, and V. Lemos, Solid State Commun. **41**, 281 (1982).

[17]R. S. Katiyar and J. D. Freire, Solid State Commun. **40**, 903 (1981).

[18]P. S. Peercy, I. J. Fritz, and G. A. Samara, J. Phys. Chem. Solids **36**, 1105 (1975).